Mechanistic studies on transcutaneous vaccine delivery : microneedles, nanoparticles and adjuvants

Bal, S.M.

Chapter 4

Influence of microneedle shape on the transport of a fluorescent dye into human skin *in vivo*

Suzanne M. Bal, Annelieke C. Kruithof, Raphaël Zwier, Ekkehart Dietz, Joke A. Bouwstra, Jürgen Lademann, Martina C. Meinke

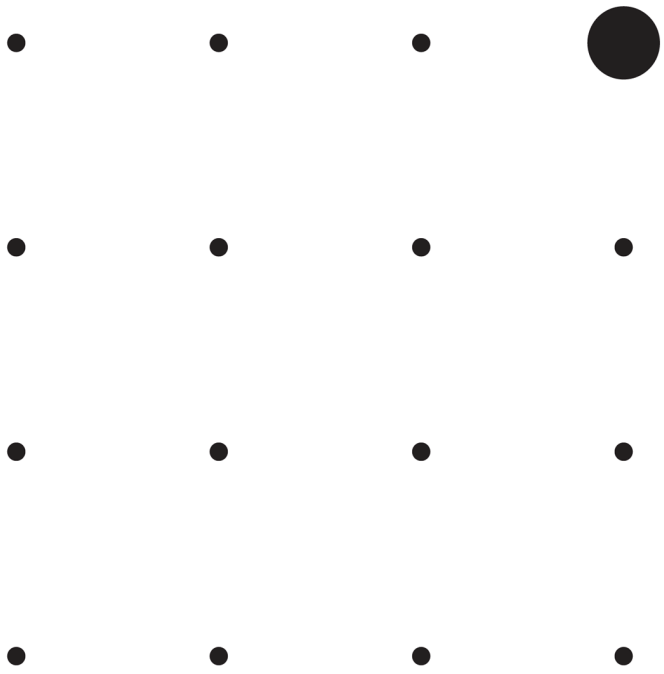

Journal of Controlled Release 2010, 147(2):218-224

Abstract

Microneedles can enhance the penetration of vaccines into the skin for transcutaneous vaccination. In this study for the first time the influence of microneedle geometry on the transport through the formed conduits was visualised on human volunteers by confocal laser scanning microscopy. Three differently shaped 300 µm long microneedle arrays were selected and fluorescein was applied either before or after piercing. Based on the intensity a distinction was made between regions with high and low intensity fluorescence (HIF and LIF). The areas of both intensities were quantified over time. In most cases HIF areas were only present in the stratum corneum, while LIF areas were also present in the viable epidermis. The areas were larger if fluorescein was applied after piercing compared to before piercing. After 15 minutes almost no HIF was present anymore at the skin surface. The microneedle geometry, but not the manner of application affected the shape and depth of the conduits. In conclusion we showed that the different microneedle arrays are able to form conduits in the skin, but the geometry of the microneedles influences the penetration of the fluorescent dye. This is the first step towards a more rational design of microneedle arrays for transcutaneous vaccination.

Introduction

Microneedles are used in the field of transcutaneous drug delivery for more than a decade [1]. They were developed as either a replacement for the traditional needle and syringe or to facilitate the transport across the skin barrier. Microneedles are shorter than traditional needles, generally less than 1 mm long, but long enough to breach the stratum corneum barrier, the upper 20 µm of the skin. Because of the elasticity of the skin, the microneedles need to have a certain length to achieve insertion into the skin [2]. This length depends on the manner of insertion, manual or with an applicator. Verbaan et al. showed that, when applied with a certain velocity, microneedles with a length of 300 µm can successfully and reproducibly pierce the skin [3]. Microneedles of this length are generally not perceived as painful [4, 5]. The application of microneedles creates small conduits in the skin. These conduits are large enough to allow penetration of high molecular weight compounds across the stratum corneum, which can not be transported into the skin passively [6]. However, compared to piercing with a conventional needle, there is only minimal microbial infiltration through the conduits and microorganisms do not reach the dermis [7]. More recently microneedles have also been used for vaccination [8-12].

Several types of microneedles have been developed. The microneedles can either be hollow or solid. Hollow microneedles can be used to inject a vaccine into the skin. This increases the bioavailability of the vaccine compared to solid microneedles, because the majority of the dose ends up in the skin. One disadvantage is the possibility of leakage to the skin surface that is expected to increase when shorter microneedles are used. Hollow microneedles have been successfully used for vaccination purposes. Recently, van Damme et al. published a clinical trial showing that a 5 times lower dose of influenza vaccine administered via the MicronJet (NanoPass Technologies), consisting of 4 hollow microneedles with a length of 450 µm, induced similar titres compared to the full dose administered intramuscularly [13]. Solid microneedle arrays can either be coated with the vaccine or used to pre-treat the skin after which a patch containing the vaccine is applied. Matriano et al showed that by coating solid microneedles with ovalbumin a 50-fold higher immune response was induced compared to intramuscular administration of the same dose in guinea pigs [11]. The most straightforward manner is to use solid microneedles to pierce the skin resulting in small conduits. Ding et al. showed a significant increase in antibody response in mice after diphtheria toxoid application on microneedle pre-treated skin in comparison to untreated skin. The application of cholera toxin as an adjuvant could amplify the titres to comparable levels as after subcutaneous immunisation [8].

Even though microneedles are a very promising tool for transcutaneous immunisation, little is known about the optimal type (hollow or solid), geometry, length and shape of the arrays. Most studies focus on the immune response generated, while the dimensions of

the formed conduits and the transport across these conduits are less well studied. A more thoroughly investigation of these parameters may allow for a rational design of microneedle arrays for transcutaneous vaccination.
Recently we showed that by using confocal laser scanning microscopy (CLSM) it is possible to visualise the conduits made by microneedle treatment in human volunteers [14]. To our knowledge this was the first time that microneedle conduits were visualised in an *in vivo* study on human volunteers. The transport of a fluorescent dye into the skin could be visualised over time. To examine the influence of the shape of the microneedles, in the present study we compared three different microneedle arrays. Two types of arrays were developed in our lab and have already proven to be painless [4] and to be able to induce enhanced immune responses [8, 15]. They were compared to the commercially available Dermastamp®. All three types of arrays consist of solid stainless steel microneedles with a length of 300 µm, but with a variable microneedle shape. We explored the behaviour of the conduits formed by these microneedles in 6 healthy subjects over time by CLSM. As a model drug fluorescein was used. To investigate if the application method had an influence on the formed conduits, the fluorescent dye was applied before and after piercing.

Materials and Methods

Volunteers

Six healthy volunteers (5 women and 1 man), aged between 20 and 58 years (mean 33 years) with no pre-existing skin conditions participated in the study. The study was approved by the Ethics Committee from the University Hospital Charité (Berlin, Germany) in accordance with the Rules of Helsinki.

Materials

Three different types of microneedle arrays were used. In figure 1 light microscopy images and schematic drawings of the microneedles are shown.

1) Assembled metal microneedle arrays (figure 1A and D) with a length of 300 µm (300A) were manufactured from commercially available 30G hypodermic needles [16]. These microneedles were positioned in a 4x4 pattern in a polymer mould (diameter 5 mm) with a pitch of 1.25 mm. The microneedles are 300 µm in diameter at the base and have a very sharp tip with an angle of 15°.
2) Stainless steel microneedles prepared by electrical discharge machining (300ED). The microneedles have a square base of 250 x 250 µm and a length of 300 µm and are also positioned in a 4x4 pattern with a pitch of 1.25 mm. The shape of the tip is defined by a diagonal plane which runs from the top of one side of the square pillar to the opposed

bottom, in this way forming an angle of approximately 40° relative to the bottom surface (figure 1B and E).

To apply these types of microneedles in a controlled manner an electrical applicator was used, as described before [16]. With this applicator the microneedles are applied onto the skin with a speed of 3 m/s.

3) These microneedles were compared to the commercially available Dermastamp® (Dermaroller S.a.r.l., Wolfenbuettel, Germany). The Dermastamp® consists of 6 microneedles (one in the center, radially surrounded by 5 others). These microneedles also have a length of 300 µm, a diameter of 120 µm and a pitch distance of 2 mm (figure 1C and F). They were applied manually three times on the same area by turning the stamp approximately 45°.

To visualise the conduits a 0.2% solution of sodium fluorescein was used (Alcon Pharma GmbH, Freiburg, Germany).

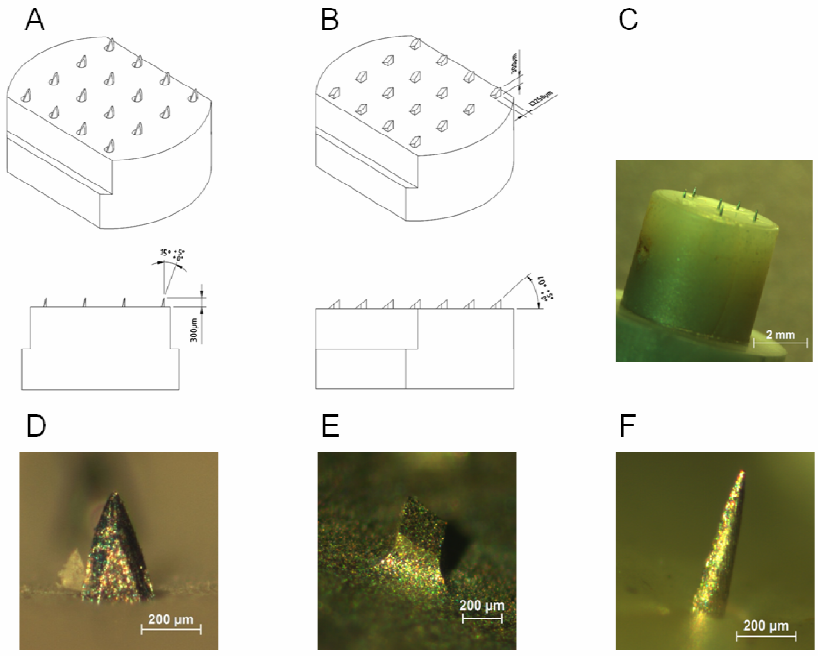

Figure 1. Images of the different microneedle arrays used in this study. A: 300A microneedle array, assembled of 30G needles. B: 300ED microneedle array made of stainless steel. C: Dermastamp® consisting of 6 microneedles. In figure D, E and F higher magnification images of single microneedles are shown.

Confocal laser scanning microscopy

The fluorescent dye in the conduits was visualised with *in vivo* confocal laser scanning microscopy (CLSM) (Stratum® System, OptiScan, Melbourne, Australia) as previously described [17]. A hand-held device containing the optical system and the focus tuning is connected to the basic station containing an Argon laser (488 nm). The measuring area is 235 x 235 µm^2 and the penetration depth of the Argon laser in human skin is about 200 µm [18]. The intensity of the laser varied between 450 and 520 µW.

Experimental procedure

The microneedles and the formulations were applied on the ventral forearms of the volunteers. The skin was disinfected before the formulations and the microneedle systems were applied. On each volunteer all three microneedle systems were tested in triplicate in a randomised order. The fluorescein solution (50 µl / 0.8 cm^2) was applied in two different manners. Either the skin was first treated with the microneedles after which the dye was applied for 1 minute, or the dye was applied before microneedle treatment. In the latter case the dye was removed immediately after microneedle treatment. Afterwards the conduit was visualised with CLSM. At 5, 10 and 15 minutes after application images were taken at different depths. At least 5 images were taken to monitor the dye at the surface, the lateral and vertical distribution and the maximal penetration depth. Between the measurements the laser was set out of focus to avoid bleaching. As a control a drop of fluorescein was applied to untreated skin. This control experiment showed that at the concentration used in this study no bleaching of the fluorescein occurred.

Data analysis

The images were analysed with respect to fluorescence pixel intensity and area using Image J (National institute of health, USA). The pixel intensity was categorised into three different classes: the class with the highest pixel intensity was set between 230 and 255 AU and the signal was referred to as high intensity fluorescence (HIF); the class with pixel intensity between 230 and 14 AU is referred to as low intensity fluorescence (LIF) and the class with pixel intensity values below 14 AU is regarded as background. The autofluorescence of the skin was always below 14 AU. These thresholds were selected based on analysing 31 random images of different depths taken from two volunteers. The thresholds were selected in such a way that at least 90% of the test pixels were inside the described classes. The fluorescent signal from other skin structures such as furrows or hair follicles was removed manually. The area of either HIF or LIF was calculated by the number of pixels in the specified intensity areas. The following parameters were analysed: the area of HIF at the surface; the maximum area of LIF in the skin and its corresponding depth; and the total depth of the conduit determined by the maximum depth where LIF can be detected. The parameters are further explained in figure 2.

Statistical analysis

The data analysis was performed considering that the measurements within one volunteer are not independent. Therefore, the statistical analysis of the univariate and the multivariate effect of the factors microneedle system, time, and application method has to

be based on random effect models. The generalised estimation equation (GEE) -method of SPSS (SPSS Inc., Chicago, Illinois) was used for statistical analysis.

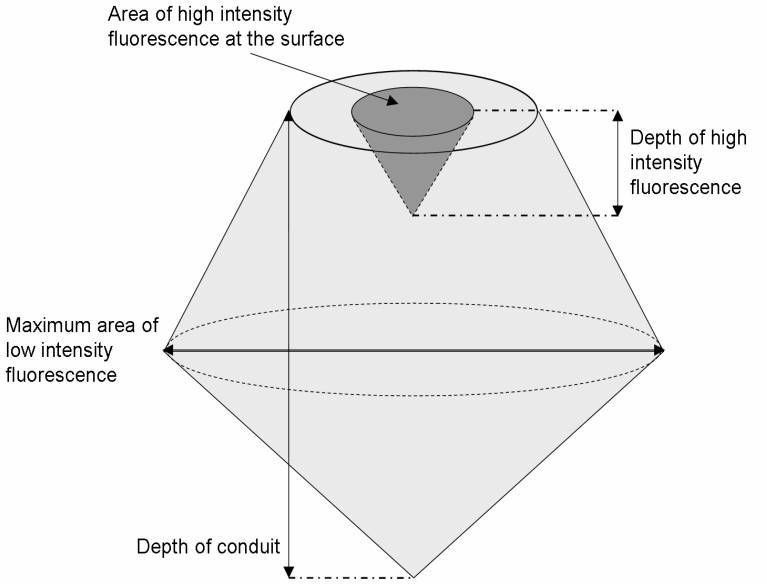

Figure 2. Schematic representation of diffusion pattern of the fluorescent dye after microneedle treatment. The grey levels represent the difference in fluorescent intensity.

Results

Adverse effects

Application of the microneedle arrays was not perceived as painful. After application with the 300A microneedles, occasionally small blood spots could be observed visually where they had pierced the skin. In those cases with the CLSM often erythrocytes could be found in the conduits. With the other types of microneedles no bleeding was detected. When small blood spots were detected, the fluorescent images were not included in the analysis.

Dimensions of the conduits formed by the different microneedle arrays

In summary, 95 conduits were investigated and 285 images were taken at different time points and at different depths. In figure 3 representative images obtained after the pre-treatment with the different microneedle arrays and subsequent dye application are shown. The differences in shape of the conduits formed by the three microneedle arrays can be observed. The images show the conduits 5 minutes after application of the fluorescent dye at different depths in the skin. The shape of the conduits was dependent on the type of microneedle array used. The 300A microneedles form half-moon shaped conduits and the dye areas are much larger than those visualised after treatment with the other two arrays. The conduits formed after application of the two other arrays are more

round-shaped and similar in size. From the images a difference in fluorescence intensity in depth can be observed. In the upper layers of the skin the bright HIF is clearly visible, while at the deeper skin layers a more diffuse low intensity signal is present. In the images taken at the surface of the skin also the shape of the corneocytes is visible. The fluorescent dye preferably diffuses through the lipid regions surrounding the corneocytes, outlining the cells. The shape of the conduits was not influenced by the method of application: applying the dye before or after piercing induced similarly shaped conduits (data not shown).

To be able to study the shape of the conduits and the diffusion of the fluorescent dye through the conduits over time, images were made at 5, 10 and 15 minutes after dye application. Figure 4 shows representative images made after application of the 300A microneedle array at different depths over time. The images obtained after treatment with the other two microneedle arrays showed comparable patterns. From these images it appears that the largest area of HIF was present at the skin surface at all time points. However, this was not always the case. In around 40 % of the cases (an example is provided in figure 5) the largest area of HIF was observed somewhat deeper in the skin, but within the upper 20 µm of the skin, the stratum corneum. This percentage differs between the arrays: for the Dermastamp® this occurred in 48% of the cases and for the 300A only in 30%. The area of HIF at the surface decreased over time and generally after 15 minutes almost no HIF could be detected at the skin surface or deeper in the conduit. In addition, figure 4 shows that the area of LIF also reduced over time. Furthermore, the depth where still fluorescence could be detected decreased over time. While after 5 and 10 minutes the LIF is still observed at a depth of 100 µm in the skin, after 15 minutes this can only be seen until a depth of 60 µm.

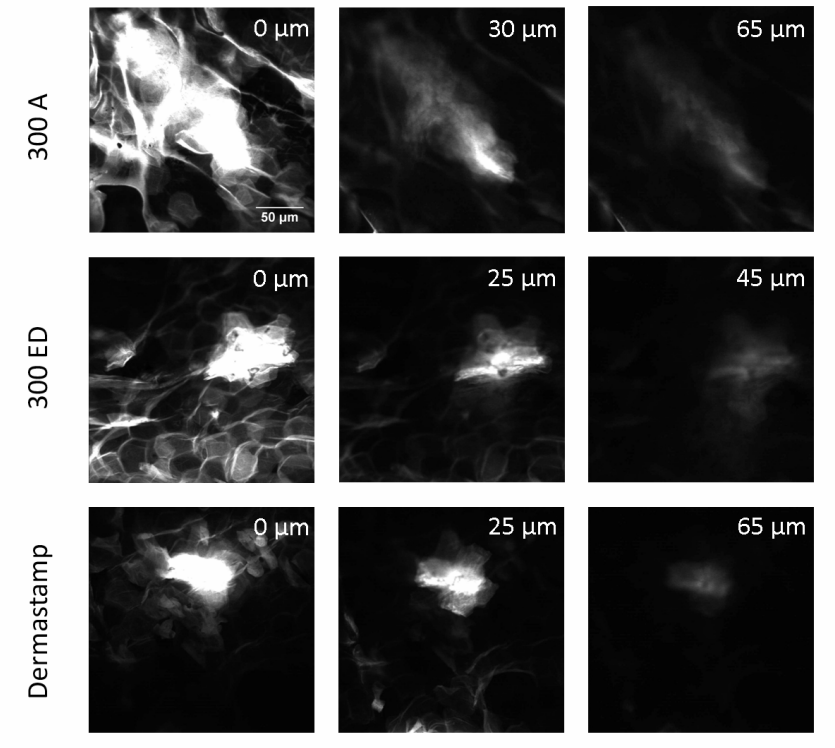

Figure 3. Representative images of the conduits formed by the different microneedle arrays after pre-treatment with the microneedles followed by application of the fluorescent dye. Images were taken 5 minutes after the application of the dye at different depths. Dimensions of the images are 235 by 235 μm^2.

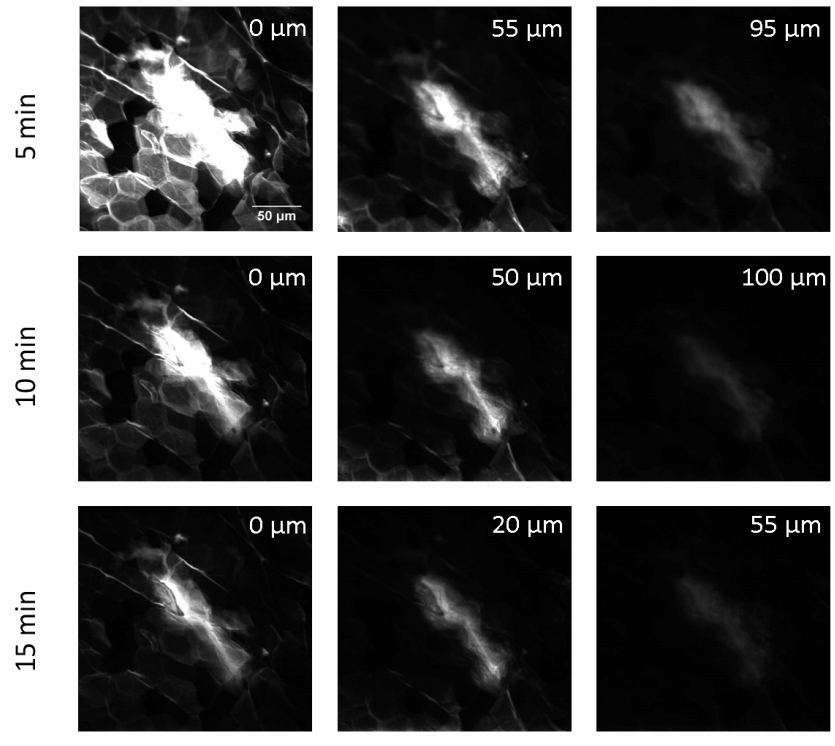

Figure 4. Representative images of a microneedle conduit formed by the 300A microneedles at different depths over time. The fluorescent dye present in the conduits can be observed. Dimensions of the images are 235 by 235 μm^2.

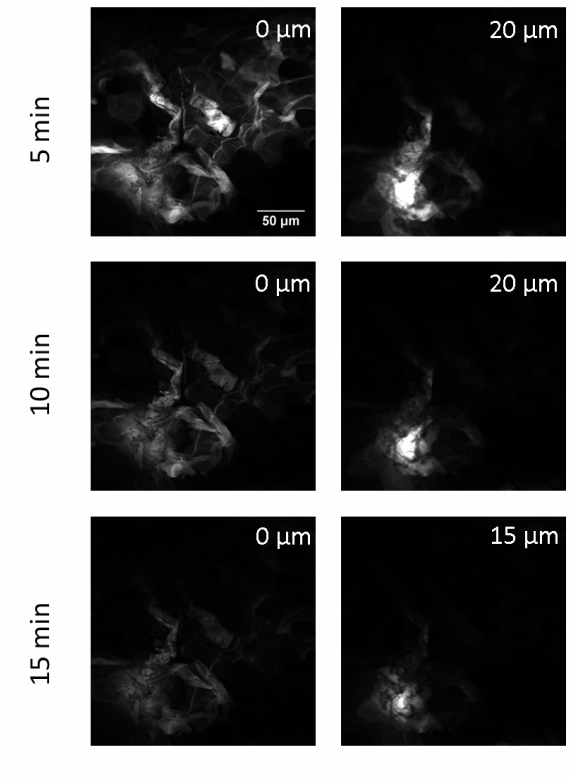

Figure 5. Selected images of a microneedle conduit formed by the Dermastamp® showing the area of HIF below the surface in the skin. The fluorescent dye present in the conduits can be observed. Dimensions of the images are 235 by 235 μm^2.

Area of HIF at the skin surface after different microneedle applications

From the images the area containing HIF present at the skin surface could be calculated. At 5 min in almost all conduits (96%) HIF appeared. After 10 min in 72% of the conduits HIF could be observed and after 15 min still 55% of the conduits showed HIF, but the area of this fluorescence strongly decreased over time ($p<0.001$). As mentioned before, the shape of the conduits was not influenced by the manner of applying the microneedle arrays. However, the area containing HIF present both at the surface and in the deeper layers of the skin was affected by the application method. In figure 6 the area containing HIF at the skin surface after both methods of microneedle application is plotted over time. The fluorescence in the furrows was not taken into account. For all arrays there is a distinct difference between piercing before or after application of the fluorescent dye (figure 6/table 1). The size of the areas was twice as large when the dye was applied after microneedle treatment ($p<0.05$). This was the case at all time points.

The differences in needle shape are reflected by the obtained areas of HIF. After piercing with the 300ED microneedles and the Dermastamp® similarly sized areas of HIF were formed at the surface which decreased over time in a comparable manner. For both methods of application, treatment with the 300A microneedles resulted in an area of HIF at the surface that was twice the size compared to those observed with the two other types of microneedle arrays ($p<0.001$). It has to be mentioned that for applying the dye

before piercing with the 300ED microneedles the data are only obtained from 3 volunteers. Because of the square shape of these 300ED microneedles, they tended to push the dye away when applied and this made it very difficult to find the conduits. Therefore it was decided to skip this application for the remaining volunteers. As a consequence for the statistical analysis comparing the two application methods only the 300A and the Dermastamp® were included. For both the 300A and the Dermastamp® a significantly larger area of HIF was present at the surface of the skin if the microneedles were used to pre-treat the skin ($p<0.05$).

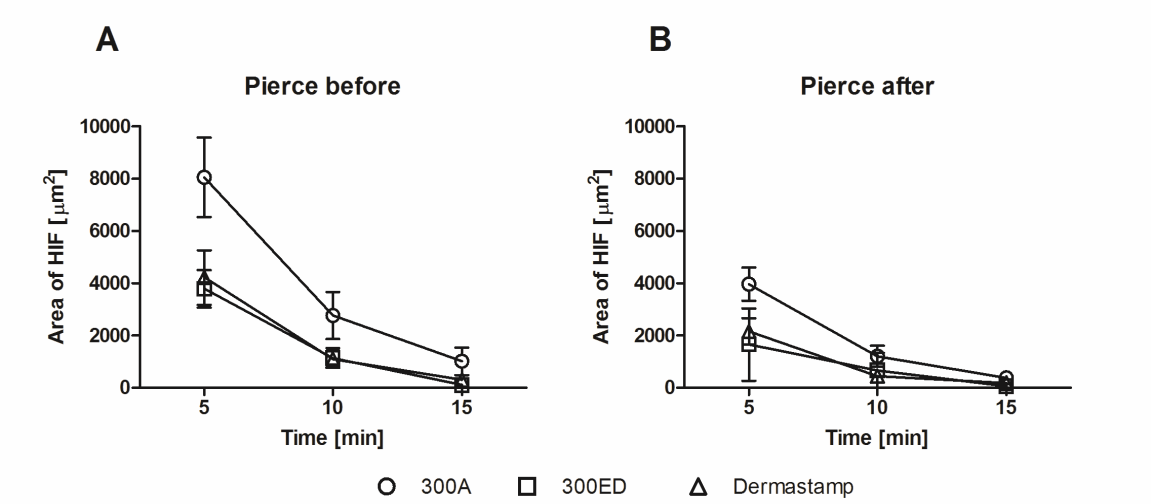

Figure 6. The area of HIF measured at the skin surface. A and B: area of HIF present at different time points on the surface of the skin when the microneedles were used to pierce either before (A) or after (B) dye application. Mean ± SEM of 6 volunteers, except for the data of piercing with the 300ED microneedles after fluorescein application which is of 3 volunteers.

Table 1. Data analysis by the GEE-method of the influence of the different microneedle arrays, application methods and time on the analysed parameters. If not mentioned otherwise only the results of piercing before dye application.

Factor	Depth of conduit	Maximum area of HIF	Maximum area of LIF
Microneedle system	***	***	***
Before and after ‡	n.s.	*	n.s.
Time	***	***	***
Interaction microneedle system – time	**	n.s.	*
Interaction before and after – time ‡	n.s.	*	n.s.

* $p<0.05$
** $p<0.01$
*** $p<0.001$
n.s . not significant
‡ Only the 300A and the Dermastamp® are taken into account.

Area of LIF in the skin

Deeper into the skin still some HIF could be observed, but mostly regions of LIF were found. In figure 7 the maximum area of LIF from the conduit (Fig 7A) and the corresponding depth (Fig 7B) at which these areas are located are shown as a function of time. Only the data of applying the fluorescein after microneedle treatment are shown. However, the data of applying the fluorescent dye before microneedle application showed the same trend.

Comparing the different microneedle arrays, the maximum area of LIF (figure 7A) showed the same trend as that of the HIF at the surface (figure 6B). The largest area of LIF can be observed after pre-treatment with the 300A microneedles ($p<0.001$), with a size approximately twice that induced by the other two arrays. The maximum areas of LIF after application of the 300ED and the Dermastamp® did not differ significantly from each other. The decrease in the size of the area of LIF over time also shows a similar profile as that of the HIF at the surface. The maximum area of LIF after application of the Dermastamp® was found deeper in the skin compared to the other two arrays ($p<0.01$). After 5 minutes the maximum area of LIF was found at the deepest location in the skin. Over time not only the size of the area, but also the depth at which the maximum LIF was located decreased ($p<0.001$).

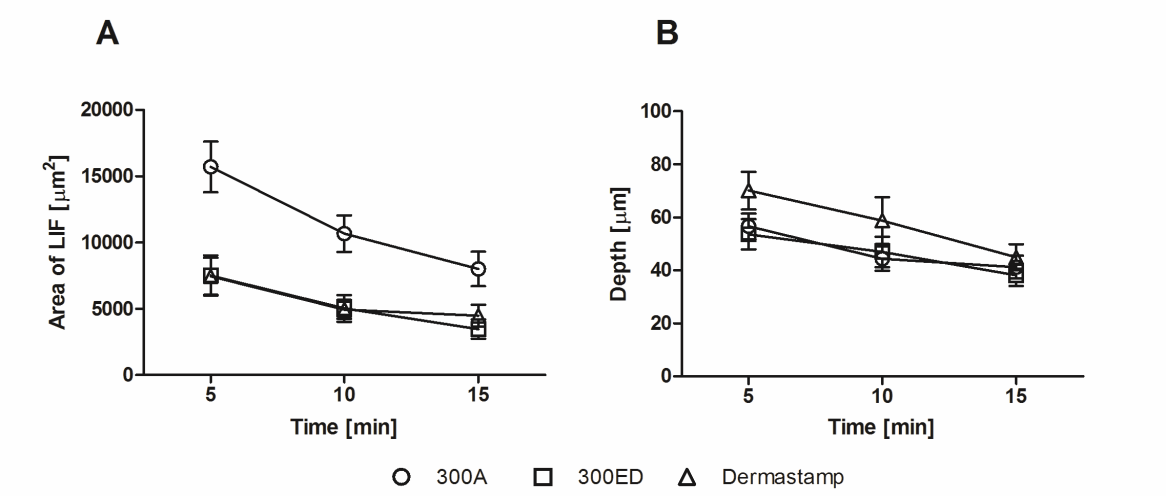

Figure 7. Maximum area of LIF when the dye is applied after microneedle treatment at different time points (A) and the corresponding depth (B) at which these areas are located. Mean ± SEM of 6 volunteers.

For all arrays also the maximum depth of the conduit was determined by the depth at which the last image was taken where LIF could still be detected. In figure 8 the data are shown of fluorescein dye application before and after microneedle treatment for the different time points. No significant differences in conduit depth between both application methods were found. After microneedle pre-treatment the deepest conduits were

observed with the Dermastamp® ($p<0.001$), which could be observed until a depth of 170 ± 13 µm into the skin. For the 300A and 300ED microneedles, LIF could be observed until 120 ± 10 µm. The depth of the conduits formed by applying the fluorescein before application did not differ between the 300A and the Dermastamp®. The depth of the conduit decreased over time, but after 15 minutes for all three microneedle arrays the LIF could still be detected at a depth of 60 µm, depending on the microneedles used.

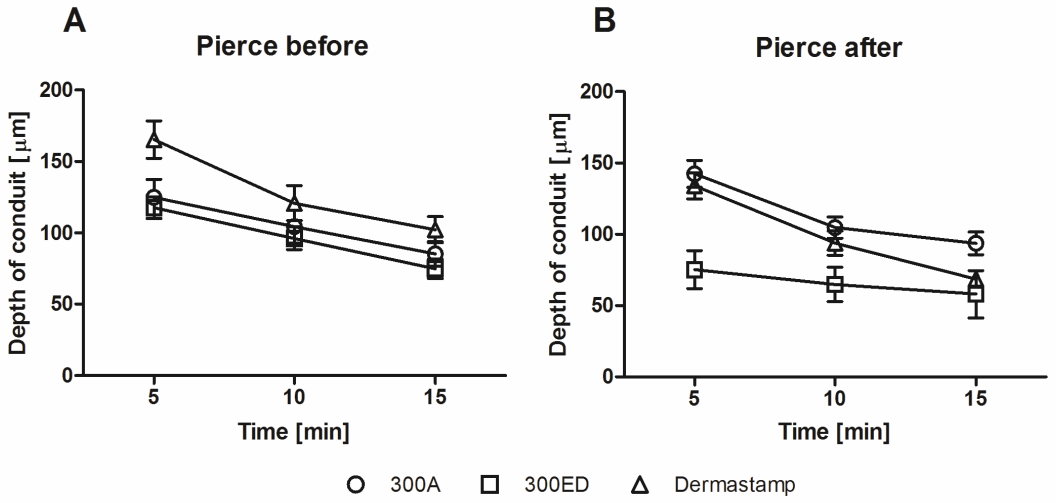

Figure 8. Total depth of the conduits formed by the three different microneedle arrays. In figure A the data of piercing before fluorescein application and in figure B that of piercing after fluorescein application is shown. Mean ± SEM of 6 volunteers, except for the data of piercing with the 300ED microneedles after fluorescein application which is of 3 volunteers.

Discussion

Microneedle based vaccination has received a lot of attention in the past years and offers great promise as a replacement for the traditionally used hypodermic needle and syringe. Advances in the mechanical field have allowed scientists to develop a great variety of microneedles, differing not only in material, but also in shape and length [6]. By means of vaccination studies information has been gained about their functionality [8-13, 19, 20], but data on the influence of microneedle shape on the conduit characteristics and the transport though the conduits is scarce.

In this study CLSM was used to visualise the conduits made by three solid, stainless steel microneedle arrays differing in microneedle shape *in vivo* in humans. CLSM provides the opportunity to gather information about the geometric parameters of the microneedle conduits by collecting images at different depths. Moreover, the behaviour of the diffusion of the fluorescent dye along the conduits over time can be studied to determine the dynamics of the transport through the conduits. Most studies performed so far are *in vitro* studies using different visualisation techniques. Coulman et al. visualised the microneedle

conduits in human epidermal membranes made by 280 µm long silicon microneedles. They used scanning electron microscopy (SEM) to show the conduit area at the skin surface and the deposition of fluorescently labelled nanoparticles in this conduit area [21]. Badran et al. used light microscopy and SEM to visualise the conduits made by the Dermaroller® *in vitro*. They showed that the size of the conduits was related to the length of the microneedles [22]. Even though with these techniques the shape of the conduits at the surface can be visualised, they do not provide information about the depth of the conduits and the transport into the skin. With CLSM it is possible to obtain insight into the transport process both *in vitro* and *in vivo* without the necessity to process the skin, as the tissue is optically sectioned. Verbaan et al. used CLSM to visualise the transport of FITC labelled polystyrene nanoparticles up to a depth of 250 µm into the skin *in vitro* after application of the 300A microneedles [3]. In another study Verma et al. also used CLSM to visualise *in vitro* the conduits made by Dermarollers® differing in microneedle length and geometry [23]. Both parameters influenced the penetration depth of DiI (1,1'-Dioctadecyl-3,3,3',3'-tetramethylindocarbo-cyanine perchlorate). All these studies provide insight into the microneedle conduit dimensions, but the need for an *in vivo* evaluation of the microneedle conduits remains.

In the present study the transport of a fluorescent dye through the conduits could be visualised *in vivo*. We showed that the shape of the microneedles influences the dimensions of the conduits. Three different microneedle arrays were used. The 300A microneedle array has already successfully been used for drug delivery and vaccination purposes [3, 8, 15, 16] and the 300ED microneedles were recently developed in our lab. The Dermastamp®, a variation on the Dermaroller®, was developed mainly for cosmetic usage, but recently also their usage for drug delivery purposes was studied [22, 23]. It has however not yet been used in vaccination studies. Even though the length of the microneedles of all three arrays was 300 µm, the 300A microneedles, with a very sharp tip and applied with an electrical applicator, formed the largest conduits. The base areas of the 300A and 300ED have a comparable size, but the tips of the 300ED microneedles have a different shape and are less sharp than the 300A microneedles. Therefore the effective area of contact between the microneedle and the skin is larger, requiring more force to penetrate the skin to a similar depth as the 300A microneedles [24]. The 300A and 300ED (4x4 arrays, 16 microneedles) are applied with an applicator, to ensure reproducible piercing. The Dermastamp® consists of 6 very sharp microneedles, of a much smaller diameter compared to the 300A (see figure 1), therefore less force was necessary for insertion into the skin [24]. This difference in microneedle diameter and number of microneedles may explain that although the deepest conduits were found after application of the Dermastamp®, only after application of the 300A microneedles occasionally minor bleeding was observed. The smaller diameter of the Dermastamp® microneedles reduces

the chance of reaching a blood vessel. In a previous study the 300A microneedles were used to study skin irritation and reduction in skin barrier [4]. In that study the 300A microneedles did not induce bleeding. Even though the application speed of the applicator was the same in both studies, in the previous study the microneedles were placed in a larger back plate. The smaller back plate used in the current study might increase the pressure applied to the skin and thereby the microneedles may pierce deeper into the skin. Most probably, by adjusting the speed of microneedle insertion, bleeding can be prevented. Even though the penetration depth of the fluorescein differed between the different microneedle applications, for all three microneedle arrays fluorescence could be detected in the epidermis, indicating successful breaching of the stratum corneum. A general limitation of the CLSM is the low sensitivity at depths larger than 150-200 µm, thereby failing to detect fluorescence intensity at this depth. The depths achieved suggest that the epidermis and to some extent the dermis is reached, which would be very useful for drug and vaccine delivery.

In previous studies TEWL measurements showed that the conduits remained open for a few hours [4, 25] under non occlusive conditions. This means that after microneedle pre-treatment drugs can be delivered through the conduits for a longer period of time. The present study shows that once the fluorescein has entered the conduits, it rapidly diffuses both in the lateral and vertical direction. Within 15 minutes a strong reduction in both high and LIF was observed indicating spreading of the dye. Control experiments were performed to determine whether bleaching plays a role in the reduced intensities over time. At the concentrations and conditions used in this study no bleaching of the fluorescein was observed (data not shown). Therefore the reduction in fluorescent intensity implies that vaccines might also be easily and rapidly transported to dendritic cells. Immunisation studies with microneedles demonstrated that an enhanced immune response can be induced by microneedle pre-treatment [8, 15]. Even though we found differences in the dye areas present in the skin between the two application methods, the maximum depth where still LIF could be detected did not differ. This means that the amount of dye that enters the conduits will end up at a similar depth in the skin. An explanation for the higher areas of both high and LIF found for piercing before dye application might be the different penetration times. When the fluorescent dye is applied prior to piercing, it was immediately removed after piercing. This means that the dye could only enter the conduits if it is being taken along with the microneedles during piercing. The penetration time for dye application after piercing was 1 minute, during which time fluorescein could migrate into the open conduit. Longer application times could reduce these differences.

It would be interesting to repeat the visualisation studies with nanoparticles, as these are often used in vaccination studies. Transport of nanoparticles through intact skin is

practically impossible. Studies have indicated that if nanoparticles are applied to intact skin they will primarily form a depot in the stratum corneum [26, 27] or remain in the hair follicles [28]. The conduits formed in this study should allow the penetration of nanoparticles into the skin, but as reviewed by Milewski *et al.* both the formulation and the pore lifetime are important parameters for successful transport into the skin [29]. By combining nanoparticles with microneedle arrays, they could reach the Langerhans cells and dendritic cells present in the epidermis and the dermis, respectively.

In conclusion, all three microneedle arrays are able to form conduits *in vivo* in human skin. The shape of the microneedles and the application speed both influence the shape and depth of the conduits that are formed. Sharp microneedles, such as present in the 300A and the Dermastamp®, are good candidates to use for transcutaneous vaccination. Whereas these studies show that microneedle sharpness and diameter affect the distribution of a fluorescent dye into the skin, other parameters, such as microneedle length, material and type, may also have a profound influence. The comparison of these parameters is necessary to draw conclusions about the ideal microneedle device.

Acknowledgements

This research was performed under the framework of TI Pharma project number D5-106-1; Vaccine delivery: alternatives for conventional multiple injection vaccines.

The authors like to thank Horst Liebl for supplying us with the Dermastamp®.

References

1. Henry S, McAllister DV, Allen MG, and Prausnitz MR, *Microfabricated microneedles: A novel approach to transdermal drug delivery.* J. Pharm. Sci., 1998. **87**(8): p. 922-925.
2. Martanto W, Moore JS, Couse T, and Prausnitz MR, *Mechanism of fluid infusion during microneedle insertion and retraction.* J. Control. Release, 2006. **112**(3): p. 357-361.
3. Verbaan FJ, Bal SM, van den Berg DJ, Dijksman JA, van Hecke M, Verpoorten H, van den Berg A, Luttge R, and Bouwstra JA, *Improved piercing of microneedle arrays in dermatomed human skin by an impact insertion method.* J. Control. Release, 2008. **128**(1): p. 80-88.
4. Bal SM, Caussin J, Pavel S, and Bouwstra JA, *In vivo assessment of safety of microneedle arrays in human skin.* Eur J Pharm Sci, 2008. **35**(3): p. 193-202.
5. Gill HS, Denson DD, Burris BA, and Prausnitz MR, *Effect of microneedle design on pain in human volunteers.* Clin J Pain, 2008. **24**(7): p. 585-594.
6. Prausnitz MR, *Microneedles for transdermal drug delivery.* Adv Drug Deliver Rev, 2004. **56**(5): p. 581-587.
7. Donnelly RF, Singh TRR, Tunney MM, Morrow DIJ, McCarron PA, O'Mahony C, and Woolfson AD, *Microneedle Arrays Allow Lower Microbial Penetration Than Hypodermic Needles In Vitro.* Pharm. Res., 2009. **26**(11): p. 2513-2522.
8. Ding Z, Verbaan FJ, Bivas-Benita M, Bungener L, Huckriede A, van den Berg DJ, Kersten G, and Bouwstra JA, *Microneedle arrays for the transcutaneous immunization of diphtheria and influenza in BALB/c mice.* J. Control. Release, 2009. **136**(1): p. 71-78.
9. Kim Y-C, Quan F-S, Yoo D-G, Compans RW, Kang S-M, and Prausnitz MR, *Improved influenza vaccination in the skin using vaccine coated microneedles.* Vaccine, 2009. **27**(49): p. 6932-8.
10. Koutsonanos DG, del Pilar Martin M, Zarnitsyn VG, Sullivan SP, Compans RW, Prausnitz MR, and Skountzou I, *Transdermal influenza immunization with vaccine-coated microneedle arrays.* PLoS One, 2009. **4**(3): p. e4773.
11. Matriano JA, Cormier M, Johnson J, Young WA, Buttery M, Nyam K, and Daddona PE, *Macroflux (R) microprojection array patch technology: A new and efficient approach for intracutaneous immunization.* Pharm. Res., 2002. **19**(1): p. 63-70.
12. Widera G, Johnson J, Kim L, Libiran L, Nyam K, Daddona PE, and Cormier M, *Effect of delivery parameters on immunization to ovalbumin following intracutaneous administration by a coated microneedle array patch system.* Vaccine, 2006. **24**(10): p. 1653-1664.
13. Van Damme P, Oosterhuis-Kafeja F, Van der Wielen M, Almagor Y, Sharon O, and Levin Y, *Safety and efficacy of a novel microneedle device for dose sparing intradermal influenza vaccination in healthy adults.* Vaccine, 2009. **27**(3): p. 454-459.
14. Bal S, Kruithof AC, Liebl H, Tomerius M, Bouwstra J, Lademann J, and Meinke M, *In vivo visualization of microneedle conduits in human skin using laser scanning microscopy.* Laser Phys Lett, 2010. **7**(3): p. 242-247.
15. Ding Z, Van Riet E, Romeijn S, Kersten GFA, Jiskoot W, and Bouwstra JA, *Immune Modulation by Adjuvants Combined with Diphtheria Toxoid Administered Topically in BALB/c Mice After Microneedle Array Pretreatment.* Pharm. Res., 2009. **26**(7): p. 1635-1643.
16. Verbaan FJ, Bal SM, van den Berg DJ, Groenink WHH, Verpoorten H, Luttge R, and Bouwstra JA, *Assembled microneedle arrays enhance the transport of compounds varying over a large range of molecular weight across human dermatomed skin.* J. Control. Release, 2007. **117**(2): p. 238-245.
17. Meyer LE and Lademann J, *Application of laser spectroscopic methods for in vivo diagnostics in dermatology.* Laser Phys Lett, 2007. **4**: p. 754-760.
18. Kandarova H, Richter H, Liebsch M, and Lademann J, *Stratum corneum architecture of reconstructed human skin models monitored by fluorescent confocal laser scanning microscopy.* Laser Phys Lett, 2007. **4**(4): p. 308-311.
19. Hirschberg H, de Wijdeven G, Kelder AB, van den Dobbelsteen G, and Kerstena GFA, *Bioneedles (TM) as vaccine carriers.* Vaccine, 2008. **26**(19): p. 2389-2397.

20. Mikszta JA, Alarcon JB, Brittingham JM, Sutter DE, Pettis RJ, and Harvey NG, *Improved genetic immunization via micromechanical disruption of skin-barrier function and targeted epidermal delivery.* Nat Med, 2002. **8**(4): p. 415.
21. Coulman SA, Anstey A, Gateley C, Morrissey A, McLoughlin P, Allender C, and Birchall JC, *Microneedle mediated delivery of nanoparticles into human skin.* Int J Pharm, 2009. **366**(1-2): p. 190-200.
22. Badran MM, Kuntsche J, and Fahr A, *Skin penetration enhancement by a microneedle device (Dermaroller (R)) in vitro: Dependency on needle size and applied formulation.* Eur J Pharm Sci, 2009. **36**(4-5): p. 511-523.
23. Verma DD and Fahr A, *Investigation on the efficacy of a new device for substance deposition into deeper layers of the skin: Dermaroller*$^{(R)}$. 2001, Institut für Pharmazeutische Technologie und Biopharmazie, Philipps-Universität Marburg.
24. Davis SP, Landis BJ, Adams ZH, Allen MG, and Prausnitz MR, *Insertion of microneedles into skin: measurement and prediction of insertion force and needle fracture force.* J Biomech, 2004. **37**(8): p. 1155-1163.
25. Banga AK, *Microporation applications for enhancing drug delivery.* Exp Opin Drug Deliver, 2009. **6**(4): p. 343-354.
26. Kuntsche J, Bunjes H, Fahr A, Pappinen A, Ronkko S, Suhonen MU, and Urtti A, *Interaction of lipid nanoparticles with human epidermis and an organotypic cell culture model.* Int J Pharm, 2008. **354**(1-2): p. 180-195.
27. Zhang LW, Yu WW, Colvin VL, and Monteiro-Riviere NA, *Biological interactions of quantum dot nanoparticles in skin and in human epidermal keratinocytes.* Toxicol Appl Pharm, 2008. **228**(2): p. 200-211.
28. Lademann J, Richter H, Teichmann A, Otberg N, Blume-Peytavi U, Luengo J, Weiss B, Schaefer UF, Lehr CM, Wepf R, and Sterry W, *Nanoparticles - An efficient carrier for drug delivery into the hair follicles.* Eur J Pharm Biopharm, 2007. **66**(2): p. 159-164.
29. Milewski M, Brogden NK, and Stinchcomb AL, *Current aspects of formulation efforts and pore lifetime related to microneedle treatment of skin.* Expert Opin Drug Deliv. **7**(5): p. 617-29.